Bull. Chem. Soc. Jpn., 73, 2553—2558 (2000)

New Organogelators Bearing Both Sugar and Cholesterol Units: an Approach toward Molecular Design of Universal Gelators

Masato Amaike, Hideki Kobayashi, and Seiji Shinkai*

Chemotransfigration Project, Japan Science and Technology Corporation (JST), 2432 Aikawa, Kurume, Fukuoka 839-0861

(Received May 24, 2000)

The gelators of organic solvents are classified into two categories on the basis of their basic intermolecular forces: hydrogen-bonded or nonhydrogen-bonded. To utilize these two interactions cooperatively for organogel formation we newly synthesized seven gelators (**1—7**) and two reference compounds (**8** and **9**) which have both a cholesterol moiety and a saccharide moiety within one molecule. The solubility of **1—7** changed drastically from totally insoluble one to very soluble one depending on the saccharide absolute configuration. In general, the gelator became very insoluble when it includes many equatorial OH groups, whereas it became very soluble when it includes many axial OH groups. Gelators **2** and **5** bearing two equatorial OH groups and one axial OH group acted as good gelators and in several cases the sol-gel phase-transition temperatures (measured in a sealed tube) were higher than the boiling points. The SEM observations of the xerogels established that the stable gels contain the entangled fibrous network. These results indicate that a very stable organogel can be designed by a cooperative coagulative effect of a cholesterol–cholesterol interaction and a saccharide–saccharide interaction.

The development of new gelators of organic solvents has recently attracted much attention. They not only gelate various organic solvents but also create novel fibrous superstructures which can be characterized by SEM observation of the xerogels.[1—18] These organogels are of particular interest in that, unlike polymer gels, fibrous aggregations of low molecular-weight compounds formed by non-covalent interactions are responsible for such gelation phenomena. Thus, the gelators can be classified into two categories according to the difference in the driving force for the molecular aggregation: viz. hydrogen-bond-based gelators and nonhydrogen-bond-based gelators. In the former category, aliphatic amide derivatives which feature efficient hydrogen-bonding interactions among the amide groups have been widely studied.[1—7] The SEM observations of these derivatives showed that various superstructures can be created by a slight difference in the intermolecular hydrogen-bonding network.[11,13,19] These results stimulated us and others to use saccharides as a hydrogen-bond-forming segment in the gelators, because one can easily introduce a variety of hydrogen-bond-forming segments (including chiral ones) into gelators by appropriate selection from a saccharide library.[11,13,20—23] Nonhydrogen-bond-based cholesterol gelators utilizing van der Waals interactions for coagulation exhibit the relatively low but broad gelation ability.[17,18] In contrast, hydrogen-bond-based gelators involving amide or saccharide moieties exhibit the strong gelation ability in aprotic solvents but the ability nearly disappears in protic solvents.[1—7] Here, it occurred to us that if one can design some gelator in which the cholesterol-cholesterol interaction can occur synergistically with the intermolecular hydrogen-bonding interaction, the resultant gelation ability should be markedly improved and appear universally both in protic and aprotic solvents. With these objects in mind we designed seven cholesterol-saccharide conjugate gelators (**1-7**), taking a combinatorial approach into account, and synthesized them according to Scheme 1. As mentioned above, saccharides can provide various intermolecular hydrogen-bonding patterns, so that some of them should show the cooperativity with the cholesterol–cholesterol interaction while some of them should not. The structures of the saccharides which we used are indicated in Table 1. Compounds **8** and **9** were also synthesized as reference compounds for **4** and **5**, respectively, which do not have the saccharide–saccharide hydrogen-bonding inter-

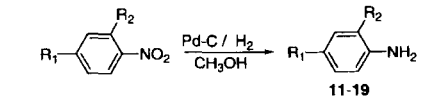

11-19

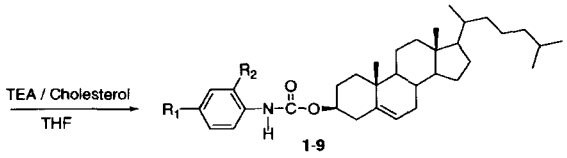

1-9

1, 11	R_1 = α-D-glucopyranosyl	R_2 = H
2, 12	R_1 = α-D-galactopyranosyl	R_2 = H
3, 13	R_1 = α-D-mannopyranosyl	R_2 = H
4, 14	R_1 = β-D-glucopyranosyl	R_2 = H
5, 15	R_1 = β-D-galactopyranosyl	R_2 = H
6, 16	R_1 = H	R_2 = β-D-glucopyranosyl
7, 17	R_1 = H	R_2 = β-D-galactopyranosyl
8, 18	R_1 = 2,3,4,6-tetra-*O*-acetyl β-D-glucopyranosyl	R_2 = H
9, 19	R_1 = 2,3,4,6-tetra-*O*-acetyl β-D-galactopyranosyl	R_2 = H

Scheme 1.

Table 1. Saccharide Chemical Structures of **1-9**

	Gelator								
	1	**2**	**3**	**4**	**5**	**6**	**7**	**8**	**9**
Saccharide moiety	Glc	Gal	Man	Glc	Gal	Glc	Gal	Glc(OAc)	Gal(OAc)
α/β	α	α	α	β	β	β	β	β	β
Secondary OH (OR) groups[a]									
equatorial	3	2	2	4	3	4	3	4	3
axial	1	2	2	0	1	0	1	0	1
Position in phenyl ring	*p*	*p*	*p*	*p*	*p*	*o*	*o*	*p*	*p*

a) Including 1-OR

action.

Results and Discussion

Gelation Test. The gelation test was carried out for 17 different solvents (Table 2). The gelator (4.0 mg) was mixed with solvent (0.10 ml) in a septum-capped test tube and the mixture was heated until the solid had dissolved. The solution was cooled to room temperature and left for 1 h (G and *G in Table 1 denote that a gel was formed at this stage). It is clearly seen from Table 2 that the solubility and the gelation ability are profoundly related to the saccharide structure appended to the cholesterol unit. Firstly, β-glucopyranoside-based **4** is insoluble in most solvents. Among 17 solvents, only aniline dissolved it, but a precipitate was formed when the solution was cooled to room temperature. The basic difference of the β-glucopyranoside skeleton from others is that all OH groups (including 1-OR) occupy the equatorial position. Since the axial OH preferably forms an intramolecular hydrogen-bond whereas the equatorial OH does not,[24] the four OH groups in **4** should be all used for the intermolecular hydrogen-bonds. This structural characteristic makes **4** extremely insoluble in most solvents.

Table 2. Organic Solvents Tested for Gelation by **1-9**[a]

	Gelator								
Organic solvent	**1**	**2**	**3**	**4**	**5**	**6**	**7**	**8**	**9**
Hexane	I	I	I	I	I	*G	I	I+G	I
Cyclohexane	P	G	Gp	I	Gp	S	I	I+G	I+G
Methylcyclohexane	P	G	Gp	I	G	S	*G	G	P
Benzene	*G	G	G	I	G	S	P	S	S
o-Xylene	P	G	G	I	S	S	P	G	S
p-Xylene	*G	G	*G	I	G	S	P	G	S
m-Xylene	P	G	G	I	S	S	P	G	S
Toluene	I	G	G	I	G	S	P	G	S
Chloroform	P	P	Gp	I	G	S	S	S	S
Chlorobenzene	*G	G	G	I	G	S	S	S	S
Ethyl acetate	I	P	Gp	I	Gp	S	*G	S	S
Aniline	Gp	G	Gp	P	G+P	S	S	G+P	S
Cyclohexanone	*G	S	Gp	I	S	S	S	S	S
Acetone	I	G+P	P	I	P	*G	*G	S	S
Methanol	I	P	P	I	P	S	P	*G	P
Acetonitrile	I	I	I	I	P	P	P	*G	*G
Water	I	I	I	I	I	I	I	I	I

a) [gelator] = 4.0 (wt/v)%; G = transparent gel, *G = turbid gel, Gp = partial gel, S = clear solution after cooling, P = precipitation, I = insoluble.

Then, why is **6** so soluble in most solvents? This is the second intriguing feature we found in Table 2. It is virtually insoluble in water and gives a precipitate from acetonitrile and the turbid gel from hexane and acetone, but is very soluble in the residual 13 solvents. Compound **6** also possesses a β-glucopyranoside skeleton and the sole difference from **4** is the substitution position in the phenyl ring (*o*- versus *p*-). We previously evaluated the aggregation mode of azobenzene-appended cholesterol-based gelators (**10**) by a computation method.[10] It was shown that when the cholesterol moieties of **10** (with naturally-occurring (*S*) C-3 configuration) form a one-dimensional stacking column, the azobenzene moieties are helically arranged, like a spiral staircase, around the cholesterol column and can enjoy a face-to-face-type interaction (Chart 1, Fig. 1).[10] This is the aggregation mode exactly occurring in **4**, in which the β-glucopyranoside moieties can efficiently interact with each other: that is, a cholesterol–cholesterol interaction occurs in a one-dimensional column and a β-glucopyranoside–β-glucopyranoside interaction occurs in a spiral staircase and the synergistic effect makes the aggregate very insoluble in most solvents. In contrast, the β-glucopyranoside group in **6** is introduced into the *o*-position. They are diverted toward various directions around the one-dimensional cholesterol column and cannot interact with each other. Thus, they cannot act synergistically with the cholesterol stacking column so much as to stabilize the one-dimensional aggregate. The similar rationale may be valid to explain the solubility difference between α-glucopyranoside-based **1** and β-glucopyranoside-based **4**. In β-anomeric **4** the phenyl-D-glucopyranoside linkage is nearly straight, whereas in α-anomeric **1** it possesses a step-like zigzag structure. The latter structure is more unfavorable to the face-to-face-type stacking aggregation. The results indicate the importance of the substitution position as well as that of the saccharide absolute configuration.

Thirdly and more importantly, compound α-galactopyran-

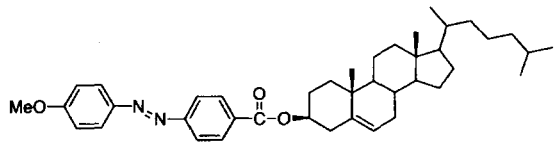

10

Chart 1. Compound **10**.

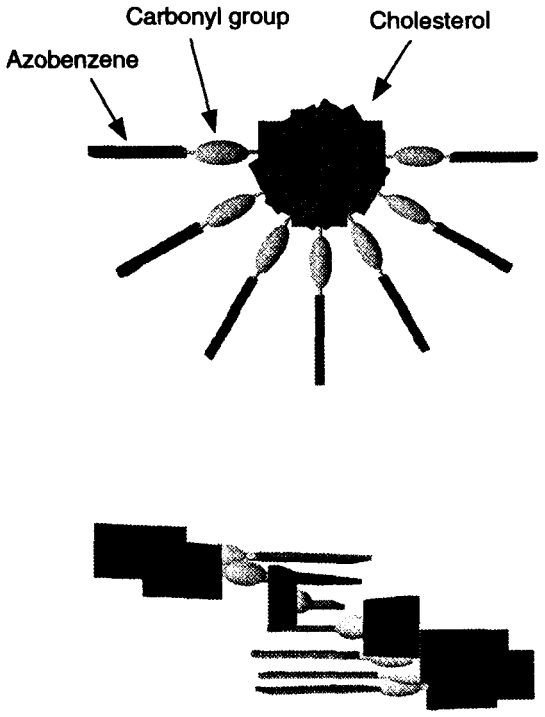

Fig. 1. Structure of **10** and the top view illustration of the one-dimensional columnar aggregate.

oside-based **2**, α-mannopyranoside-based **3**, and β-galactopyranoside-based **5** act as good gelators of many organic solvents. In particular, **2** can gelate 9 solvents out of 17 solvents. The structural features common to these three gelators are (i) the saccharide groups are all introduced into the *p*-position and (ii) they possess at least one free axial OH group. Provided that this axial OH group is used for the formation of an intramolecular hydrogen-bond (as described above), the residual OH groups useful for the formation of intermolecular hydrogen-bonds are 2. This number may provide the "moderate" saccharide–saccharide interaction or facilitate the growth of the one-dimensional hydrogen-bonding array indispensable to gel fiber formation.[24] In **4** with three free equatorial OH groups available for the formation of intermolecular hydrogen-bonds, the saccharide-saccharide interaction may be too strong or the hydrogen-bonding network may grow up to either the two-dimensional or the three-dimensional direction which is unfavorable to gelation.[24]

Sol-Gel Phase-Transition Temperature. We measured the sol–gel phase-transition temperatures (T_{gel}) in order to obtain quantitative insights into the "cooperativity" in the gel formation mechanism. The results are summarized in Table 3. The T_{gel} values are relatively high; very surprisingly, those for several samples are comparable with or even higher than the boiling points: e.g., **1**+benzene gel (T_{gel} 80 °C), **2**+cyclohexane gel (T_{gel} 80 °C), **5**+methylcyclohexane, benzene, and chloroform gels (T_{gel} 100 °C, 101 °C, and 80 °C, respectively). Such high T_{gel} values have never been achieved with simple cholesterol- or saccharide-based gelators. These results suggest that the gel fiber network in these organogel systems is cooperatively stabilized

Table 3. Sol–Gel Phase-Transition Temperatures (T_{gel})[a)]

		Gelator						
Organic solvent	bp °C	**1**	**2**	**3**	**4**	**5**	**6**	**7**
Hexane	69						51	
Cyclohexane	81		80					
Methylcyclohexane	101		93			100		46
Benzene	80	80	64	55		101		
o-Xylene	144		65	52				
p-Xylene	138	106	76	100		100		
m-Xylene	139		70	57				
Toluene	111		66	54		101		
Chloroform	61					80		
Chlorobenzene	132	105	80	36		101		
Ethyl acetate	77							75
Aniline	185		55					
Cyclohexanone	156	60						
Acetone	56						55	25

a) [gelator] = 4.0 (wt/v)%.

by both cholesterol-cholesterol and saccharide–saccharide interactions. We tentatively plotted T_{gel} against the ratio of equatorial OH (OR)/axial OH (OR) in Fig. 2. Gelator **5** with three equatorial substituents and one axial one can provide very stable organogels, but can gelate only a limited number of organic solvents. On the other hand, **2** with two equatorial and two axial substituents can gelate many solvents, but the organogels are not so stable at high temperature. This counterbalance teaches us one essential factor governing the "gelation ability": that is, a coagulative molecule tends to precipitate and is not suitable to be a gelator, but once it is oriented into the one-dimensional direction in its specific solvent, it can provide a very stable organogel.

Compounds **8** and **9** were synthesized as reference compounds for **4** and **5**, which cannot form the intermolecular

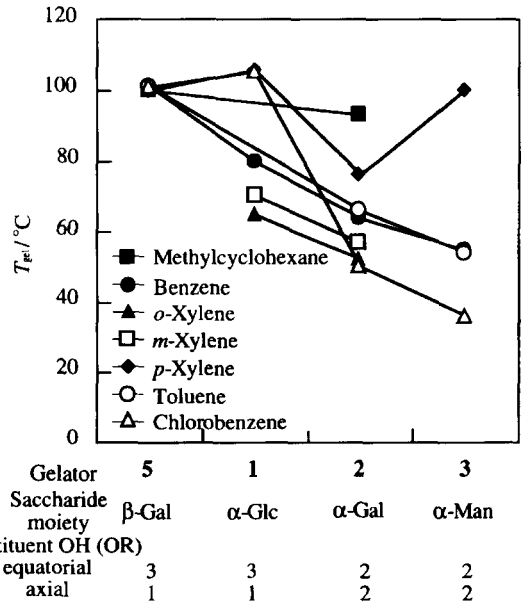

Fig. 2. Correlation between T_{gel} and saccharide absolute configration.

hydrogen-bond (except the urethane group[25]). As expected, **9** is soluble in most organic solvents. In contrast, **8** gelates several organic solvents, although the T_{gel} values are not so high as those for **2**, **3**, and **5**. Presumably, the molecular shape of **8** is very suitable to the one-dimensional molecular stacking using a van-der-Waals-type interaction. In **4**, this energetically-favorable molecular stacking is further intensified by intermolecular hydrogen-bonds. This is why **4** is very insoluble in most solvents, because of two strong coagulative forces.

SEM Observations of Xerogels. To obtain visual images of the organogel systems, we took SEM pictures of xerogels obtained from the *p*-xylene gels of **2**, **3**, and **5** (Fig. 3). The **3**+*p*-xylene gel, which is a little turbid but has been classified into a stable gel with T_{gel} 100 °C, showed a network structure with fiber diameters of 50—90 nm (Fig. 3B). On the other hand, the **2**+*p*-xylene gel, which is translucent but has been classified into a less stable gel with T_{gel} 76 °C, showed a lamellar structure with some fibers only on the edge of the lamellae (Fig. 3A). The difference clearly indicates that the origin of the organogel stabilization is related to the entanglement of fibrous one-dimensional aggregates in the solution. The **5**+*p*-xylene gel, which is translucent but has been classified into a stable gel with T_{gel} 100 °C, showed a lamellar structure (Fig. 3C).

SEM pictures of xerogels obtained from the cyclohexane gels of **8** and **9** were also taken (Fig. 4). The **9**+cyclohexane gel provided straight fibers which are scarcely entangled with one another at all. The diameters of the fibers are relatively large (0.5—1.0 μm). On the other hand, the **8**+cyclohexane gel showed the typical network structure suitable to the gelation. The fiber diameters are relatively small (40—60 nm). The difference again supports the importance of the fibrous aggregate formation for gelation.

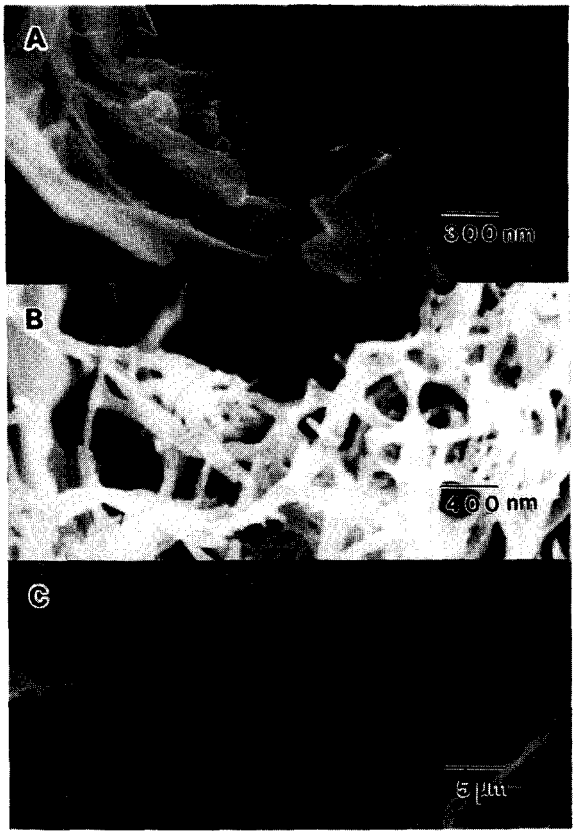

Fig. 3. SEM images of the xerogels obtained from the *p*-xylene gels of (A) **2**, (B) **3**, and (C) **5**.

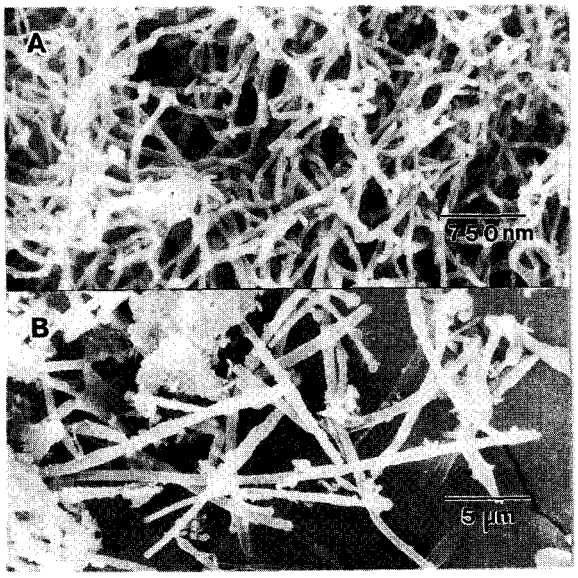

Fig. 4. SEM images of the xerogels obtained from the cyclohexane gels of (A) **8** and (B) **9**.

Conclusion

The gelators of organic solvents have so far been classified into two categories, hydrogen-bonded ones and nonhydrogen-bonded ones. To the best of our knowledge, however, there are few attempts to combine these two forces in order to develop robust organogels. To achieve this, both the cholesterol-cholesterol interaction and the saccharide–saccharide interaction must operate cooperatively in the process of organogel fiber formation. It is extremely difficult, however, to predict how the OH groups in the saccharide moiety will form the intermolecular hydrogen-bonds. We have solved this problem by a combinatorial method and we tested seven different cholesterol-saccharide conjugates. As a result, we could find a few robust gelators in which the two interactions can behave cooperatively. It is a big surprise that their sol–gel phase-transition temperatures are higher than their boiling points. One may conclude, therefore, that the selected cholesterol-saccharide conjugates can act as excellent gelators and the combinatorial approach is very helpful to find them.

Experimental

4-Aminophenyl α-D-Glucopyranoside (11): 4-Nitrophenyl α-D-glucopyranoside (603 mg, 2.0 mmol) was added to methanol (60 ml) and the solution was stirred until the solid was dissolved. Then, 10% Pd–C (60 mg) was added to the solution. Hydrogen gas was introduced into the mixed solution for 3 h at room temperature under a nitrogen atmosphere. The reaction mixture was filtered to

remove Pd–C and the filtrate was evaporated in vacuo to dryness. Compound **11** was obtained as a white powder: Yield 95%, mp 168.1—168.8 °C; IR (KBr) ν_{max} 3364, 3335, 2967, 2924, 1516, 1371, 1252, 1029, 1140, 1107, 1028, 1013, 902 cm^{-1}; ^1H NMR (DMSO-d_6) δ = 3.16—3.61 (m, 6H), 4.46 (t, J = 5.5 Hz, 1H), 4.70 (s, 2H), 4.88—4.93 (m, 3H), 5.05 (d, J = 3.6 Hz, 1H), 6.48 (d, J = 6.9 Hz, 2H), 6.78 (d, J = 6.9 Hz, 2H).

Related compounds (**12—17**) were synthesized according to a similar method. We thus describe only their analytical data.

4-Aminophenyl α-D-Galactopyranoside (12): Yield 84%, mp 161.1—161.8 °C; IR (KBr) ν_{max} 3389, 2934, 1510, 1219, 1080, 1028, 972 cm^{-1}; ^1H NMR (DMSO-d_6) δ = 3.15—3.77 (m, 6H), 4.45—4.69 (m, 6H), 5.06 (s, 1H), 6.47 (d, J = 8.6 Hz, 2H), 6.78 (d, J = 8.6 Hz, 2H).

4-Aminophenyl α-D-Mannopyranoside (13): Yield 85%; mp 157.9—159.6 °C; IR (KBr) ν_{max} 3393, 3330, 2940, 1514, 1219, 1122, 1097, 1049, 1024, 970 cm^{-1}; ^1H NMR (DMSO-d_6) δ = 3.16—3.61 (m, 6H), 3.76 (S, 1H), 4.33 (s, 1H), 4.74—4.89 (m, 6H), 5.05 (s, 1H), 6.47 (d, J = 8.6 Hz, 2H), 6.77 (d, J = 8.6 Hz, 2H).

4-Aminophenyl α-D-Glucopyranoside (14): Yield 98%, mp 162.3—162.9 °C; IR (KBr) ν_{max} 3369, 2869, 1639, 1510, 1397, 1224, 1074, 1044, 1014, 833 cm^{-1}; ^1H NMR (DMSO-d_6) δ = 3.10—3.20 (m, 4H), 3.40—3.48 (m, 1H), 3.64—3.70 (m, 1H), 4.54 (d, J = 7.1 Hz, 1H), 4.57 (d, J = 7.5 Hz, 1H), 4.71 (s, 2H), 4.95 (d, J = 5.0 Hz, 1H), 5.02 (d, J = 4.5 Hz, 1H), 5.20 (d, J = 4.8 Hz, 1H), 6.48 (d, J = 8.8 Hz, 2H), 6.76 (d, J = 8.8 Hz, 2H).

4-Aminophenyl β-D-Galactopyranoside (15): Yield 94%, mp 168.5—169.4 °C; IR (KBr) ν_{max} 3445, 3356, 2957, 1641, 1509, 1396, 1225, 1084, 1064, 1037, 885 cm^{-1}; ^1H NMR (DMSO-d_6) δ = 3.15—3.66 (m, 6H), 4.43 (d, J = 4.0 Hz, 1H), 4.53 (d, J = 7.6 Hz, 1H), 4.58—4.62 (m, 1H), 4.66 (s, 2H), 4.78 (d, J = 5.6 Hz, 1H), 5.05 (d, J = 5.0 Hz, 1H), 6.47 (d, J = 8.7 Hz, 2H), 6.75 (d, J = 8.7 Hz, 2H).

2-Aminophenyl β-D-Glucopyranoside (16): Yield 98%, mp 187.4—187.8 °C; IR (KBr) ν_{max} 3369, 2869, 1734, 1698, 1607, 1541, 1456, 1253, 1225, 1197, 1072, 1041 cm^{-1}; ^1H NMR (DMSO-d_6) δ = 3.14—3.18 (m, 4H), 3.45—3.51 (m, 1H), 3.68—3.73 (m, 1H), 4.51 (d, J = 7.1 Hz, 1H), 4.58 (t, J = 5.8 Hz, 1H), 4.95 (s, 2H), 5.01 (d, J = 5.1 Hz, 1H), 5.08 (d, J = 3.7 Hz, 1H), 5.53 (d, J = 3.7 Hz, 1H), 6.47 (t, J = 6.5 Hz, 1H), 6.63 (d, J = 7.8 Hz, 1H), 6.75 (d, J = 7.3 Hz, 1H), 6.99 (d, J = 7.7 Hz, 1H).

2-Aminophenyl β-D-Galactopyranoside (17): Yield 94%, mp 201.4—202.4 °C; IR (KBr) ν_{max} 3445, 3357, 2869, 1734, 1698, 1607, 1541, 1456, 1254, 1225, 1051 cm^{-1}; ^1H NMR (DMSO-d_6) δ = 3.39—3.58 (m, 5H), 3.69 (s, 1H), 4.47—4.51 (m, 2H), 4.65 (d, J = 5.2 Hz, 1H), 4.86 (d, J = 3.5 Hz, 1H), 4.97 (s, 2H), 5.41 (d, J = 2.5 Hz, 1H), 6.45 (d, J = 7.3 Hz, 1H), 6.74 (t, J = 7.3 Hz, 1H), 6.76 (d, J = 7.3 Hz, 1H), 6.98 (d, J = 7.5 Hz, 1H).

4-Aminophenyl-2,3,4,6-tetra-*O*-acetyl β-D-Glucopyranoside (18): Peracetylation of 4-nitrophenyl β-D-glucopyranoside was performed by treatment with pyridine and acetic anhydride. The nitrophenyl group was converted to the aminophenyl group with H_2/Pd–C: Yield 84%, mp 67.3—68.9 °C; IR (KBr) ν_{max} 3463, 3376, 2984, 1750, 1630, 1512, 1221, 1076 cm^{-1}; ^1H NMR ($CDCl_3$) δ = 2.05, 2.06, 2.10, 2.11 (s, 12H), 3.55 (s, 2H), 3.77—3.87 (m, 1H), 4.17 (d, J = 12.3 Hz, 1H), 4.31 (dd, J = 12.3 Hz, 5.1 Hz, 1H), 4.92 (d, J = 7.3 Hz, 1H), 5.13—5.5.29 (m, 3H), 6.62 (d, J = 8.8 Hz, 2H), 6.85 (d, J = 8.8 Hz, 2H).

4-Aminophenyl-2,3,4,6-tetra-*O*-acetyl β-D-Galactopyranoside (19): Compound **19** was prepared from 4-Nitrophenyl β-D-galactopyranoside by a method similar to that for **18:** Yield 85%, mp 134.2—135.2 °C; IR (KBr) ν_{max} 3480, 3386, 2951, 2868, 1756, 1741, 1624, 1514, 1375, 1224, 1211, 1076, 1045 cm^{-1}; ^1H NMR ($CDCl_3$) δ = 2.01, 2.06, 2.09, 2.18 (s, 12H), 3.54 (s, 2H), 3.98 (t, J = 6.5 Hz, 1H), 4.12—4.23 (m, 2H), 4.87 (d, J = 8.0 Hz, 1H), 5.08 (dd, J = 10.5 Hz, 3.4 Hz, 1H), 5.41—5.47 (m, 2H), 6.61 (d, J = 8.8 Hz, 2H), 6.84 (d, J = 8.8 Hz, 2H).

3β-Cholest-5-en-3-yl *N*-[4-(α-D-Glucopyranosyl)phenyl]carbamate (1): To a solution of **11** in distilled THF (90 ml) were added 3β-Cholest-5en-3-yl chloroformate (435 mg, 1.10 mmol) and triethylamine (336 mg, 3.31 mmol) under a nitrogen atmosphere. After the mixture was stirred at 60 °C for 4 h, the reaction mixture was filtrated to remove any precipitate, and the filtrate was evaporated in vacuo to dryness. The residue was purified by column chromatography on silica gel with THF/chloroform (3 : 1 v/v). Compound **1** was obtained as a white solid: Yield 84%, mp 228.3—229.7 °C; IR (KBr) ν_{max} 3351, 2950, 2868, 1701, 1604, 1514, 1468, 1217, 1109, 1076, 1025, 925 cm^{-1}; ^1H NMR (DMSO-d_6) δ = 0.64—2.40 (m, 43H), 3.16—3.22 (m, 1H), 3.46 (d, J = 8.6 Hz, 2H), 3.55—3.62 (m, 3H), 4.45—4.48 (m, 2H), 4.90 (d, J = 4.9 Hz, 1H), 4.96 (d, J = 5.7 Hz, 1H), 5.01 (d, J = 6.2 Hz, 1H), 5.25 (d, J = 3.2 Hz, 1H), 5.38 (s, 1H), 6.99 (d, J = 8.7 Hz, 2H), 7.34 (d, J = 8.7 Hz, 2H), 9.45 (s, 1H); m/z 682 $[M-H]^-$. Found: C, 69.96; H, 8.95; N, 2.00%. Calcd for $C_{40}H_{61}NO_4$: C, 70.25; H, 8.99; N, 2.05%.

Related compounds (**2-9**) were synthesized according to a similar method. We thus describe only their analytical data.

3β-Cholest-5-en-3-yl *N*-[4-(α-D-Galactopyranosyl)phenyl]carbamate (2): Yield 58%, mp 178.6—179.7 °C; IR (KBr) ν_{max} 3323, 2950, 2869, 1732, 1700, 1603, 1516, 1437, 1311, 1215, 1117, 1071, 1032, 957 cm^{-1}; ^1H NMR (DMSO-d_6) δ = 0.65—2.50 (m, 43H), 3.35—3.77 (m, 1H), 3.47—3.62 (m, 1H), 3.69—3.77 (m, 4H), 4.40—4.45 (m, 1H), 4.50 (d, J = 5.0 Hz, 1H), 4.52 (d, J = 5.9 Hz, 1H), 4.69 (d, J = 3.1 Hz, 1H), 4.81 (d, J = 4.4 Hz, 1H), 5.26 (s, 1H), 5.37 (s, 1H), 6.98 (d, J = 8.7 Hz, 2H), 7.33 (d, J = 8.7 Hz, 2H), 9.44 (s, 1H); m/z 682 $[M-H]^-$. Found: C, 69.66; H, 8.92; N, 2.01%. Calcd for $C_{40}H_{61}NO_4$: C, 70.25; H, 8.99; N, 2.05%.

3β-Cholest-5-en-3-yl *N*-[4-(α-D-Mannopyranosyl)phenyl]carbamate (3): Yield 77%, mp 167.4—168.9 °C; IR (KBr) ν_{max} 3363, 2950, 2869, 1734, 1603, 1516, 1458, 1418, 1311, 1215, 1121, 1013, 980, 830 cm^{-1}; ^1H NMR (DMSO-d_6) δ = 0.66—2.43 (m, 43H), 3.42—3.48 (m, 2H), 3.57—3.62 (m, 3H), 3.79 (s, 1H), 4.42—4.44 (m, 2H), 4.72 (d, J = 5.9 Hz, 1H), 4.80 (d, J = 5.1 Hz, 1H), 4.96 (d, J = 4.3 Hz, 1H), 5.24 (s, 1H), 5.38 (s, 1H), 6.99 (d, J = 8.7 Hz, 2H), 7.34 (d, J = 8.7 Hz, 2H), 9.46 (s, 1H); m/z 682 $[M-H]^-$. Found: C, 70.01; H, 8.98; N, 2.01%. Calcd for $C_{40}H_{61}NO_4$: C, 70.25; H, 8.99; N, 2.05%.

3β-Cholest-5-en-3-yl *N*-[4-(β-D-Glucopyranosyl)phenyl]carbamate (4): Yield 92%, mp 262.4—263.2 °C; IR (KBr) ν_{max} 3569, 3382, 2950, 1694, 1607, 1551, 1514, 1469, 1321, 1235, 1105, 1057, 1019, 831 cm^{-1}; ^1H NMR (DMSO-d_6) δ = 0.66—2.41 (m, 43H), 3.16—3.46 (m, 5H), 3.68 (d, J = 11.8 Hz, 1H), 4.42—4.47 (m, 1H), 4.55 (s, 1H), 4.74 (d, J = 7,2 Hz, 1H), 5.01 (s, 1H), 5.07 (s, 1H), 5.28 (s, 1H), 5.38 (s, 1H), 6.94 (d, J = 8.8 Hz, 2H), 7.37 (d, J = 8.8 Hz, 2H), 9.45 (s, 1H); m/z 682 $[M-H]^-$. Found: C, 70.29; H, 9.02; N, 2.08%. Calcd for $C_{40}H_{61}NO_4$: C, 70.25; H, 8.99; N, 2.05%.

3β-Cholest-5-en-3-yl *N*-[4-(β-D-Galactopyranosyl)phenyl]carbamate (5): Yield 79%, mp 219.6—220.2 °C; IR (KBr) ν_{max} 3358, 2950, 2867, 1701, 1603, 1514, 1468, 1312, 1217, 1140, 1055, 949, 833 cm^{-1}; ^1H NMR (DMSO-d_6) δ = 0.65—2.41 (m, 43H), 3.38—3.68 (m, 6H), 4.40—4.44 (m, 1H), 4.48 (d, J = 4.3 Hz, 1H), 4.63 (s, 1H), 4.71 (d, J = 7.6 Hz, 1H), 4.84 (d, J = 5.3 Hz, 1H),

5.13 (d, J = 5.0 Hz, 1H), 5.38 (s, 1H), 6.94 (d, J = 9.0 Hz, 2H), 7.33 (d, J = 9.0 Hz, 2H), 9.45 (s, 1H); *m/z* 682 $[M-H]^-$. Found: C, 69.93; H, 9.00; N, 2.02%. Calcd for $C_{40}H_{61}NO_4$: C, 70.25; H, 8.99; N, 2.05%.

3β-Cholest-5-en-3-yl *N*-[2-(β-D-Glucopyranosyl)phenyl]-carbamate (6): Yield 92%, mp 152.1—153.2 °C; IR (KBr) ν_{max} 3391, 2950, 2869, 1734, 1698, 1607, 1541, 1456, 1334, 1253, 1225, 1198, 1072, 1042 cm^{-1}; ^1H NMR (DMSO-d_6) δ = 0.66—2.45 (m, 43H), 3.45—3.70 (m, 6H), 4.47—4.54 (m, 1H), 4.49 (d, J = 5.2 Hz, 1H), 4.55 (d, J = 5.2 Hz, 1H), 4.65 (d, J = 3.7 Hz, 1H), 4.67 (d, J = 6.8 Hz, 1H), 4.91 (d, J = 5.6 Hz, 1H), 5.39 (s, 1H), 5.63 (d, J = 4.0 Hz, 1H), 6.96 (d, J = 4.0 Hz, 1H), 6.98 (d, J = 5.5 Hz, 1H), 7.09 (t, J = 3.8 Hz, 1H), 7.83 (t, J = 4.0 Hz, 1H), 8.68 (s, 1H); *m/z* 682 $[M-H]^-$. Found: C, 69.96; H, 8.93; N, 2.02%. Calcd for $C_{40}H_{61}NO_4$: C, 70.25; H, 8.99; N, 2.05%.

3β-Cholest-5-en-3-yl *N*-[2-(β-D-Galactopyranosyl)phenyl]-carbamate (7): Yield 74%, mp 174.7—175.8 °C; IR (KBr) ν_{max} 3421, 2950, 1734, 1687, 1607, 1532, 1456, 1375, 1254, 1227, 1196, 1086, 1042 cm^{-1}; ^1H NMR (DMSO-d_6) δ = 0.67—2.45 (m, 43H), 3.41—3.71 (m, 6H), 4.45—4.54 (m, 2H), 4.67 (d, J = 7.6 Hz, 2H), 4.89 (s, 1H), 5.40 (s, 1H), 5.62 (d, J = 3.4 Hz, 1H), 6.97 (d, J = 5.2 Hz, 1H), 6.98 (d, J = 4.3 Hz, 1H), 7.11 (t, 1H), 7.85 (t, 1H), 8.68 (s, 1H); *m/z* 682 $[M-H]^-$. Found: C, 70.20; H, 8.97; N, 2.01%. Calcd for $C_{40}H_{61}NO_4$: C, 70.25; H, 8.99; N, 2.05%.

3β-Cholest-5-en-3-yl *N*-[4-(2,3,4,6-Tetra-*O*-acetyl β-D-glucopyranosyl)phenyl]carbamate (8): Yield 59%, mp 205.4—205.9 °C; IR (KBr) ν_{max} 3335, 2950, 2869, 1751, 1717, 1605, 1549, 1512, 1375, 1217, 1140, 912, 841 cm^{-1}; ^1H NMR ($CDCl_3$) δ = 0.68—2.41 (m, 55H), 3.82—3.85 (m, 1H), 4.16 (dd, J = 12.3 Hz, 2.1 Hz, 1H), 4.30 (dd, J = 12.3 Hz, 5.4 Hz, 1H), 4.31 (d, J = 5.4 Hz, 1H), 5.16—5.41 (m, 4H), 6.84 (s, 1H), 6.95 (d, J = 9.0 Hz, 2H), 7.30 (d, J = 9.0 Hz, 2H); *m/z* 850 $[M-H]^-$. Found: C, 67.90; H, 8.22; N, 1.70%. Calcd for $C_{48}H_{69}NO_{12}$: C, 67.66; H, 8.16; N, 1.64%.

3β-Cholest-5-en-3-yl *N*-[4-(2,3,4,6-Tetra-*O*-acetyl β-D-galactopyranosyl)phenyl] carbamate (9): Yield 84%, mp 199.5—200.0 °C; IR (KBr) ν_{max} 3366, 2868, 1755, 1603, 1541, 1514, 1373, 1217, 1076, 1053, 955, 837 cm^{-1}; ^1H NMR ($CDCl_3$) δ = 0.70—2.52 (m, 55H), 4.02—4.27 (m, 3H), 4.57—4.65 (m, 1H), 4.98 (d, J = 8.0 Hz, 1H), 5.12 (dd, J = 10.5 Hz, 3.3 Hz, 1H), 5.42—5.52 (m, 3H), 6.52 (s, 1H), 6.97 (d, J = 8.8 Hz, 2H), 7.32 (d, J = 8.8 Hz, 2H); *m/z* 850 $[M-H]^-$. Found: C, 67.35; H, 8.16; N, 1.67%. Calcd for $C_{48}H_{69}NO_{12}$: C, 67.66; H, 8.16; N, 1.64%.

Solvent Effect on Gelation. The gelators and the solvent were put in a septum-capped sample tube and heated until the solid was dissolved. The solution was cooled at room temperature for 1 h. If the gel existed stably, it was classified as "G" or "*G". The former denotes a transparent gel, whereas the latter denotes a turbid gel.

Gel–Sol Phase-Transition Temperatures. The test tube containing the gel was immersed in a thermostatted oil bath. The temperature was raised at a rate of 2 °C min^{-1}. Here, T_{gel} is defined as the temperature at which the gel disappears.

SEM Observations. A Hitachi S-14500 scanning electron microscope was used for taking the SEM pictures. The thin gel was prepared in a sample tube and frozen in liquid nitrogen. The frozen specimen was evaporated by a vacuum pump for 24 h. The dry sample was coated by palladium-platinum. The accelerating voltage of SEM was 5—15 kV, and the emission current was 10 μA.

Miscellaneous. Column chromatography was performed on silica gel (Wako gel® C-300). Melting points were determined on a Micro Melting Point Apparatus Yanaco MP-500D. ^1H NMR spectra were measured on a Bruker ARX 300 apparatus. IR spectra were obtained in KBr pellets using a Shimadzu FT-IR 8100 spectrometer, and MS spectra were obtained by a Hitachi M-2500 mass spectrometer.

References

1 K. Hanabusa, K. Okui, K. Karaki, and H. Shirai, *J. Chem. Soc., Chem. Commun.*, **1992**, 1371 and references cited therein.

2 K. Hanabusa, Y. Yamada, M. Kimura, and H. Shirai, *Angew. Chem., Int. Ed. Engl.*, **35**, 1949 (1992).

3 K. Hanabusa, K. Shimura, K. Hirose, M. Kimura, and H. Shirai, *Chem. Lett.*, **1996**, 885.

4 K. Hanabusa, A. Kawakami, M. Kimura, and H. Shirai, *Chem. Lett.*, **1997**, 191.

5 E. J. De Vries and R. M. Kellogg, *J. Chem. Soc., Chem. Commun.*, **1993**, 238.

6 M. Takafuji, H. Ihara, C. Hirayama, H. Hachisako, and K. Yamada, *Liquid Cryst.*, **18**, 97 (1995).

7 J.-E. S. Sohna and F. Fages, *J. Chem. Soc., Chem. Commun.*, **1997**, 327.

8 E. Otsumi, P. Kamasas, and R. G. Weiss, *Angew. Chem., Int. Ed. Engl.*, **35**, 1324 (1996) and references cited therein.

9 P. Terech, I. Furman, and R. G. Weiss, *J. Phys. Chem.*, **99**, 9558 (1995) and references cited therein.

10 K. Murata, M. Aoki, T. Suzuki, T. Hanada, H. Kawabata, T. Komori, F. Ohseto, K. Ueda, and S. Shinkai, *J. Am. Chem. Soc.*, **116**, 6664 (1994) and references cited therein.

11 R. H. Hafkamp, M. C. Feiters, and R. J. M. Nolte, *J. Org. Chem.*, **64**, 412 (1999).

12 T. D. James, K. Murata, T. Harada, K. Ueda, and S. Shinkai, *Chem. Lett.*, **1994**, 273.

13 S. W. Jeong, K. Murata, and S. Shinkai, *Supramol. Sci.*, **3**, 83 (1996).

14 S. W. Jeong and S. Shinkai, *Nanotechnology*, **8**, 179 (1997).

15 T. Brotin, R. Utermöhlen, F. Fagles, H. Bouas-Laurent, and J.-P. Desvergne, *J. Chem. Soc., Chem. Commun.*, **1991**, 416.

16 J. van Esch, S. De Feyter, R. M. Kellogg, F. De Schryver, and B. L. Feringa, *Chem. Eur. J.*, **3**, 1238 (1997).

17 For a recent comprehesive review see: P. Terech and R. G. Weiss, *Chem. Rev.*, **97**, 3133 (1997).

18 S. Shinkai and K. Murata, *J. Mater. Chem.* (*Feature Article*), **8**, 485 (1998).

19 It is considered, however, that the hydrogen-bond complementarity in the gel network is more disordered than that in the crystal.[13,14]

20 S. Yamasaki and H. Tsutsumi, *Bull. Chem. Soc. Jpn.*, **69**, 561 (1996) and references cited therein.

21 M. Svaan and T. Anthonsen, *Acta Chem. Scand.*, **B40**, 119 (1986).

22 K. Yoza, Y. Ono, K. Yoshihara, T. Akao, H. Shinmori, M. Takeuchi, S. Shinkai, and D. N. Reinhoudt, *Chem. Commun.*, **1998**, 907.

23 N. Amanokura, K. Yoza, H. Shinmori, S. Shinkai, and D. N. Reinhoudt, *J. Chem. Soc., Perkin Trans. 2*, **1998**, 2585.

24 R. Luboradzki, O. Gronwald, M. Ikeda, S. Shinkai, and D. N. Reinhoudt, *Angew. Chem., Int. Ed.*, in press.

25 Recently, Weiss et al. proposed on the basis of IR spectral measurements that the intermolecular hydrogen-bonding interaction among the urethane groups scarcely contributes to the organogel stabilization: L. Lu, T. M. Cocker, R. E. Bachman, and R. G. Weiss, *Langmuir*, **16**, 20 (2000).